

1 2 3 4 5 6 7 8 9 10 11 12 13 14 15 16 17 18 19 20 21 22 23 24  
 25 26 27 28 29 30 31 32 33 34 35 36 37 38 39 40

著者（英）	山田 太郎    山田 次郎    山田 三郎    山田 四郎    山田 五郎
山田 太郎    山田 次郎    山田 三郎    山田 四郎    山田 五郎	山田 太郎    山田 次郎    山田 三郎    山田 四郎    山田 五郎
山田 太郎	山田
山田 次郎	山田
山田 三郎	山田
山田 四郎	山田
山田 五郎	山田

doi: 10.1109/TBME.2015.2504998(<http://dx.doi.org/10.1109/TBME.2015.2504998>)

# Wearable ECG Based on Impulse Radio Type Human Body Communication

Jianqing Wang, *Member, IEEE*, Takuya Fujiwara, Taku Kato, and Daisuke Anzai, *Member, IEEE*

**Abstract**—Human body communication (HBC) provides a promising physical layer for wireless body area networks (BANs) in healthcare and medical applications because of its low propagation loss and high security characteristics. In this study, we developed a wearable electrocardiogram (ECG) which employs impulse radio (IR) type HBC technology for transmitting vital signals on the human body in a wearable BAN scenario. The HBC-based wearable ECG has two excellent features. First, the wide band performance of the IR scheme contributed to very low radiation power so that the transceiver is easy to satisfy the extremely weak radio laws which does not need a license. This feature can provide big convenience in the use and spread of the wearable ECG. Second, the realization of common use of sensing and transmitting electrodes based on time sharing and capacitive coupling largely simplified the HBC-based ECG structure and contributed to its miniaturization. To verify the validity of the HBC-based ECG, we evaluated its communication performance and ECG acquisition performance. The measured bit error rate (BER), smaller than  $10^{-3}$  at 1.25 Mbps, showed a good physical layer communication performance, and the acquired ECG waveform and various heart rate variability (HRV) parameters in time and frequency domains exhibited good agreement with a commercially available radio-frequency (RF) ECG and a Holter ECG. These results sufficiently showed the validity and feasibility of the HBC-based ECG for healthcare applications. This should be the first time to have realized a real time ECG transmission by using the HBC technology.

**Index Terms**—Wearable electrocardiogram (ECG), human body communication (HBC), impulse radio transceiver.

## I. INTRODUCTION

Today's aging population is leading to a wide-scale demand for health-state monitoring in hospital and at home. Wireless health-state monitoring can effectively reduce the inconvenience of wire links, and save time and resources. As a typical usage, the wireless device is a vital sign sensor with communication function for collecting blood presser, electrocardiogram (ECG), electroencephalogram (EEG), and so on. By attaching such devices to a human body, the vital sign data can be automatically collected and transmitted to an access point via wireless body area network (BAN), and then sent to the backbone network via local area network (LAN) or cellular network, and finally forwarded to medical staff in a hospital or medical center for medical and healthcare administration and applications [1]-[3].

The wireless techniques in a wearable BAN may employ 400 MHz band, 2.4 GHz band, ultra wide band (UWB),

and human body communication (HBC) band [1]. Because of the rapid spread of the 400 MHz and 2.4 GHz transceiver integrated circuits (ICs), most existing wearable ECGs are employing these two frequency bands [4]-[8]. For example, a 433 MHz frequency shift keying (FSK) transmitter was used for sending the ECG signal to a personal computer (PC) for health-state monitoring in [5], and a 2.4 GHz Bluetooth based wireless ECG with a built-in automatic warning function was equipped in an intelligent telecardiology healthcare system in [6]. Also using the 2.4 GHz band, a wireless steering wheel was developed for fast and noninvasive ECG monitoring in [7]. The commercial transceiver ICs at 2.4 GHz is especially easy to get for wearable ECG use [8]. However, the on-body propagation mechanism depends on the working frequency. As described in [2], above 400 MHz, more than 80% received signal components are contributed by the on-body surface propagation. Since the human body is a lossy dielectric body, the higher the frequency is, the larger the on-body path loss should be. Compared to the 2.4 GHz band or UWB, however, the HBC usually operates at frequencies from dozens of kHz to dozens of MHz by employing the human body itself as a communication route [9]-[12]. At these frequencies the on-body path loss is smaller than 2.4 GHz and UWB. Its propagation along the human body is also much superior to that through the air. So HBC provides a new possibility for wireless health-state monitoring. Not only its low propagation loss may yield a superior communication performance compared to other frequency bands, but also its low radiation toward outside of the human body may bring to a high security. These features are especially important in healthcare and medical applications.

Fig. 1 shows a promising application of HBC in monitoring health-states. Some vital sign sensors are set on the human body to collect the vital data such as blood presser, blood glucose, ECG, EEG and electrooculography (EOG), and the collected data are sent to an access point in the front of the body by HBC technology automatically. In general, it is not necessary to acquire various vital data at the same time. When there are multiple sensors on the human body, the sensors can sample the data at different timing and then send them to the access point with a time division multiplexing scheme. After re-arranging these data with appropriate header into one frame in the access point, we can send out them from the access point to an HBC receiver (Rx) in one touch. The access point may be equipped in a tablet or a smart phone with HBC function. And the receiver for touch can be connected to a PC. These data in the PC can be further sent to a hospital or medical center via networks. If there is only one sensor, for example,

Manuscript received January xx, 2015; revised xx xx, 2015. This study is supported in part by JSPS KAKENHI (Grant No. 15H04006).

J. Wang, T. Fujiwara, T. Kato and D. Anzai are with the Graduate School of Engineering, Nagoya Institute of Technology, Nagoya 466-8555, Japan (e-mail: wang@nitech.ac.jp)

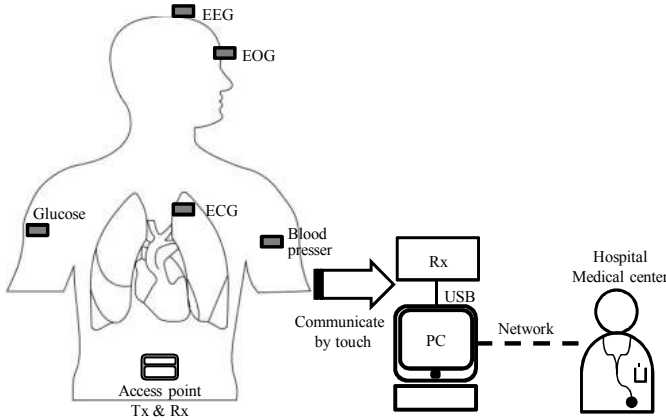


Fig. 1. Scenario of HBC based BAN for health-state monitoring. All the wearable devices have both sensing and HBC functions.

only the ECG sensor, we can remove the access point and send the data from the wearable ECG directly to the receiver which is connected to the PC.

Another promising application is to monitor a driver's health-state for safe driving [2][7]. In this scenario, some vital sign sensors are set on the driver's body to collect signals such as ECG and pulse rate. The ECG sensor may be embedded in the driver's seat belt, and the access point may be embedded in the steering wheel so that the driver unconsciously wears the sensors and send the data to the access point by HBC technology. The car's control unit can then analyze the driver's health-state data collected in the access point and generate warning signs or take automatic control of car, if necessary.

In this study, we develop a wearable ECG with HBC technology for data transmission. The HBC technology usually employs narrow band modulation schemes such as FSK or on-off keying (OOK) which yield a low data rate in the order of kbps. We employed the HBC technology with impulse radio (IR) scheme [13]. Instead of a sinusoid signal, digitized ECG data are modulated with wide band pulse signals between 10 and 60 MHz. Such a wide band transmission can provide advantages such as high data rate and anti-interference features. Its low power density also contributes to less electromagnetic absorption in human body.

This paper is organized as follows. Chapter II describes the structure of the HBC-based wearable ECG. Chapter III presents the communication performance of the developed HBC transceiver, and Chapter IV verifies the validity of the transmitted ECG signals by comparison them with that acquired by commercial ECG units. Chapter V concludes this paper.

## II. STRUCTURE OF HBC-BASED WEARABLE ECG

Fig. 2 shows the structure of our developed HBC-based wearable ECG. The ECG electrodes are composited of two 3 cm × 3 cm copper plates. The two electrodes are attached to the chest directly for ECG signal sensing. A ground electrode is further attached to the human body as a reference. The ECG signals acquired by the two sensing electrodes are

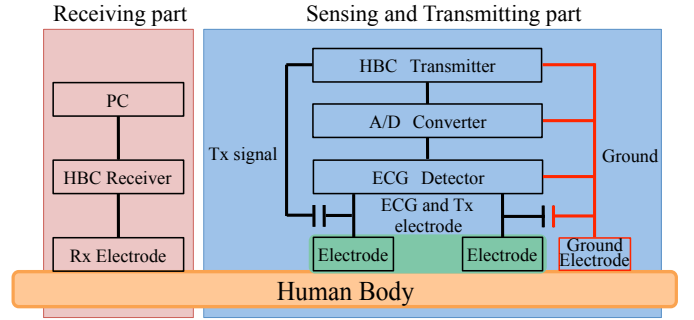


Fig. 2. Structure of HBC-based wearable ECG.

filtered and differentially amplified in the ECG detector, and then converted to digital signals by an analog-to-digital (AD) converter. The AD-converted ECG signals are transmitted by the HBC transmitter to a HBC receiver through the human body. The HBC receiver has a universal serial bus (USB) interface via which the received ECG signals are sent to a PC or tablet for data display and analysis.

As shown in Fig. 2, the two electrodes are used for not only ECG signal acquisition but also HBC transmission, i.e., they also act as the transmitting electrodes. The common use of the sensing electrodes and transmitting electrodes contributes largely to the miniaturization of the wearable ECG. When the two electrodes are used for ECG signal sensing, both of them act as the signal electrodes. While the two electrodes are used for HBC transmission, one of them acts as signal transmission and the other one acts as the ground. So the two electrodes have different potentials, depending on they act as the sensing electrodes or transmitting electrodes. We therefore cannot connect them directly to both the ECG detector and the HBC transmitter. To solve this problem, we first connect the two electrodes to the ECG detector, and then connect them to the HBC transmitter via capacitive coupling by inserting two capacitors. This makes the direct current (DC) potential of the ECG electrodes differ from that of the transmitting electrodes, and thus realize the common use of the two electrodes for both ECG sensing and HBC transmission.

### A. ECG Detector

Fig. 3 shows the block diagram of the ECG detector. The most important frequency components of an ECG signal are approximately in the range of 0.1 - 100 Hz [4]. So the ECG signals acquired from the two sensing electrodes are first filtered by two high pass filters (HPF) respectively with a cutoff frequency of 15.9 Hz. This cutoff frequency was chosen to remove effectively the DC and drift noise components without obvious degradation on the ECG signal waveform. Then two low pass filters (LPF) with a cutoff frequency of 1 MHz are used respectively to remove high frequency interferences especially from the HBC signals. In the third stage the voltage followers are used to increase the input impedance, and in the fourth stage the signals are amplified differentially around 56 dB with an operational amplifier (opamp) because the ECG signal is in the order of several mV while the AD converter

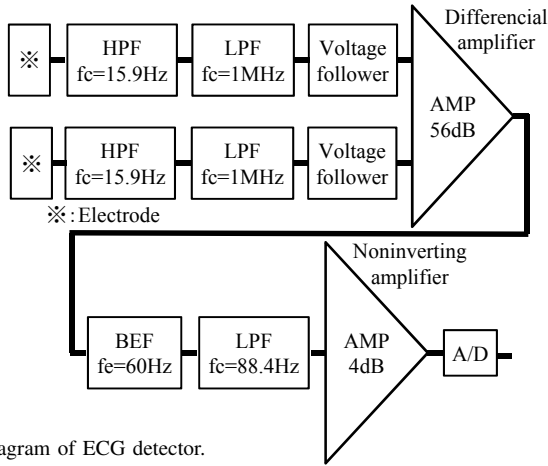


Fig. 3. Block diagram of ECG detector.

requires an input voltage of several volts. After the notch filter used for cutting the commercial power frequency of 50 or 60 Hz, a LPF with a cutoff frequency of 88.4 Hz is further used to extract effectively the ECG signals. Finally, the signal level is adjusted by an opamp to fall into the analog input range of the AD converter. The AD converter samples the analog ECG signals with a frequency of 500 Hz and quantization level of 10 bits, and the AD-converted digital ECG signals are sent to the HBC transmitter for data transmission.

### B. HBC Transceiver

Fig. 4 shows the block diagram of the IR-type HBC transmitter and receiver. The vital data such as ECG are first digitized by the AD converter. The digitized data are then modulated with wide band pulses based on IR scheme in the transmitter. The transmitting pulses are produced with a width of 100  $\mu$ s. Every hexadecimal data from 0 to F (four bits) with a data rate of 1.25 Mbps are encoded and represented by a 32-chip pseudo-noise (PN) code with a chip rate of 10 Mcps. It means that 16 different PN codes are used to represent the hexadecimal 0 to F, respectively. The pulse is sent when the chip is "1", and nothing is sent when the chip is "0". This is actually an encoded on-off keying (OOK) modulation scheme in which every eight chips (pulses) represents one bit. The corresponding data rate is thus 1.25 Mbps. The pulse's spectrum shape is formed by an appropriate band pass filter. Its main spectrum components range from 10 to 60 MHz. Under the same signal to noise power ration (SNR), the IR pulse position modulation (PPM) may provide a higher data rate compared to IR OOK [14] because it employs twice frequency bandwidth. However, if we set them to have the same bandwidth, the data rate of IR PPM is only the half of IR OOK. Therefore, whether the IR PPM has a higher data rate depends on the bandwidth to be used [2]. From the viewpoint of  $E_b/N_0$ , i.e., the energy per bit versus the noise power density, the BER performances between the IR OOK and IR PPM are actually the same. Why we chose IR OOK is due to that it may provide a higher data rate at a specified bandwidth

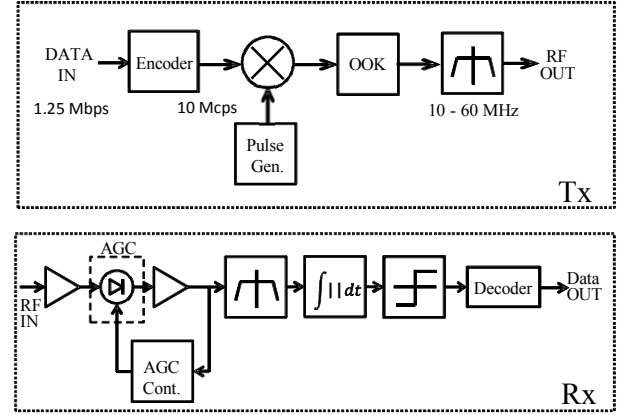


Fig. 4. Block diagram of HBC transmitter and receiver.

as well as its simpler modulation/demodulation structure.

We first measured the modulated pulse waveform and signal spectrum at the transmitter output using a spectrum analyzer. As shown in Fig. 5, the maximum signal level is found to be -15 dBm and most of the signal powers are between 10 and 60 MHz. In this frequency range, Japanese law has defined a category: extremely weak radio stations [15]. As long as the radiated electric field intensity is below 500  $\mu$ V/m or 54 dB $\mu$ V/m at a distance of three meters from the transceiver, a license is not needed for the transceiver. Fig. 6 shows the measured maximum electric field intensity as a function of frequency for our IR-type HBC transceiver in an anechoic chamber. It shows that the wide band IR transceiver structure contributes significantly to a low electromagnetic radiation to the environment, and therefore weak interference to other information and communication devices.

The HBC receiver employs an envelope detector for demodulation. The received signal is filtered and amplified, and is then adjusted to an adequate level by an automatic gain controller (AGC). After the envelope detector, the signal is judged as chip "1" or "0" by a comparator. Then in the decoder, each 32 chips were compared with the 16 different PN codes used in the encoder, respectively. The PN code which has the most agreement with the demodulated chips is determined as the sent code, and then the corresponding four-bit data are determined as the transmitted data.

Table I summarizes the basic specifications of the IR-type HBC transceiver. The transmitter was packaged on a 3 cm  $\times$  3 cm printed circuit board (PCB). The digital circuit part was implemented in a commercially available field programmable gate array (FPGA, Xilinx Spartan-6). The signal electrode was mounted on the top of the PCB, and the PCB's ground plane acted as the ground electrode. On the other hand, the receiver was packaged on a 3 cm  $\times$  10 cm PCB. A USB interface was incorporated in the receiver for being easy to send the data to a PC or other information devices.

### C. Common Use of Sensing and Transmitting Electrodes

In general, two electrodes at least are required for ECG signal sensing, and another two electrodes are required for

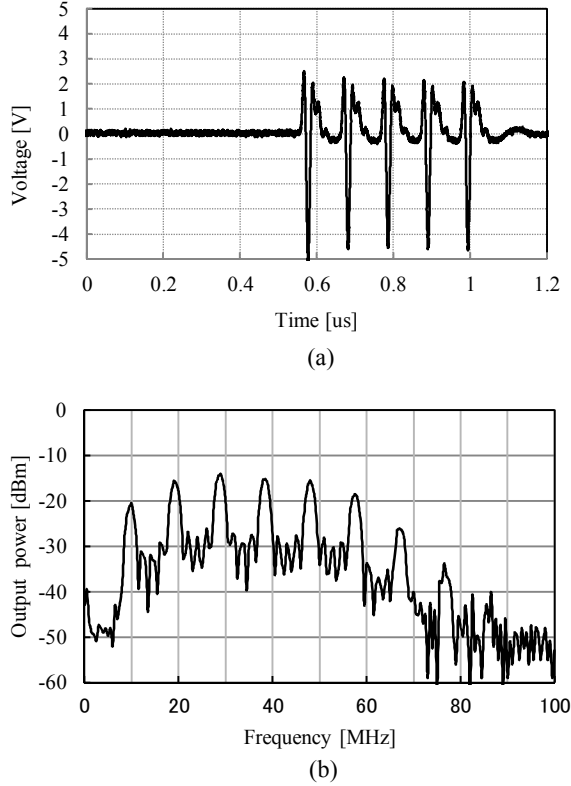


Fig. 5. (a) Example of time waveform of transmitted pulses; (b) signal spectrum at the transmitter output.

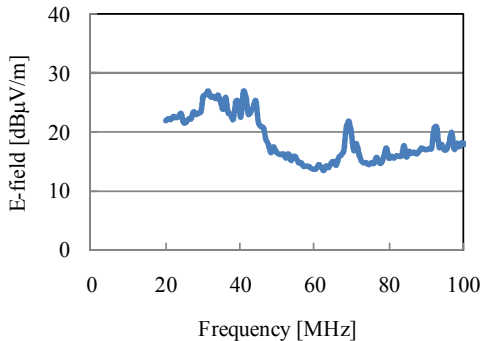


Fig. 6. Measured radiated electric field intensity in an anechoic chamber at a distance of 2.5 meter from the IR-type HBC transceiver.

HBC data transmission. To simplify such a structure, we developed a technology to share the sensing and transmitting using only two electrodes. In our HBC-based wearable ECG, the sampling frequency of ECG signal is 500 Hz so that the sampling period is 2 ms. In view of the 10 bit quantization of the AD converter, the 10 bits should be transmitted within 2 ms. On the other hand, our HBC transmitter has a data rate as high as 1.25 Mbps. With such a high data rate the transmission of one sample (10 bits) only takes 8  $\mu$ s. This make the time sharing of the two electrodes acting as either sensing electrodes or transmitting electrodes available.

Fig. 7 shows the time chart for the common use of the two

TABLE I  
IR TRANSCEIVER SPECIFICATIONS

Pulse width	100 $\mu$ s
Chip rate	10 Mcps
Chip number per bit	8
Encoder	16 different PN codes
Data rate	1.25 Mbps
Frequency band	10 - 60 MHz
Modulation	IR OOK
Maximum output	-15 dBm
Demodulation	Envelope detection
Decoder	Most agreement PN code by chip comparison
Consumption power	4.8 mW

electrodes. The sampling period  $T$  is divided into  $T_{Sensing}$ ,  $T_{HBC}$  and the rest. Within the period  $T_{Sensing}$ , the two electrodes act as sensing electrodes for the ECG detector, while within the period  $T_{HBC}$ , the two electrodes act as transmitting electrodes for the HBC transmitter. The rest period may act as a guard interval. Since the AD sampling and data transmitting do not work simultaneously, the common use of the electrodes is available. However, as mentioned previously, there is a problem in DC potential for the common use of the two electrodes. The zero potential in the ground electrode will make the acquisition of ECG signal impossible. To solve the DC potential problem in the common use of electrodes, we inserted two capacitors of 0.1  $\mu$ F, respectively, as shown in Fig. 2, to make their DC potential be different. Then during the ECG signal sensing, the two electrodes act both as the signal electrodes, while during the HBC transmission, one of them (the left electrode in Fig. 2) acts as signal electrode, and the other (the right electrode in Fig. 2) acts as the ground electrode. This is because that the right electrode is connected to the ground electrode through the capacitor of 0.1  $\mu$ F, and the impedance between the right electrode and the ground electrode is only 0.05  $\Omega$  at the center frequency of 35 MHz of the HBC communication signal. So during the HBC transmission, the right electrode is almost shorted to the ground electrode which is connected to the HBC transmitter ground. On the other hand, during the ECG detection, the capacitor of 0.1  $\mu$ F makes the right electrode and the ground electrode be cut to have different DC potentials. By the adoption of the above-described time sharing and capacitive coupling, we realized the common use of two electrodes and therefore simplified the wearable ECG structure. Moreover, the LPFs in the ECG detector were also designed to avoid the mixture of the HBC pulses into the ECG signals.

In addition, the distance between the two electrodes is set at 4 cm in our wearable ECG. This distance affects the acquired ECG waveform shape, but no significant degradation on the HBC communication performance was observed when we changed this distance up to the chest width.

### III. COMMUNICATION PERFORMANCE EVALUATION

To clarify the communication performance of the HBC transceiver, we first investigated path loss characteristics for on-body signal transmission. In [16] we have found that the path loss is around 70 - 80 dB on the entire upper part of a human body at 30 MHz. It means that the IR transceiver must

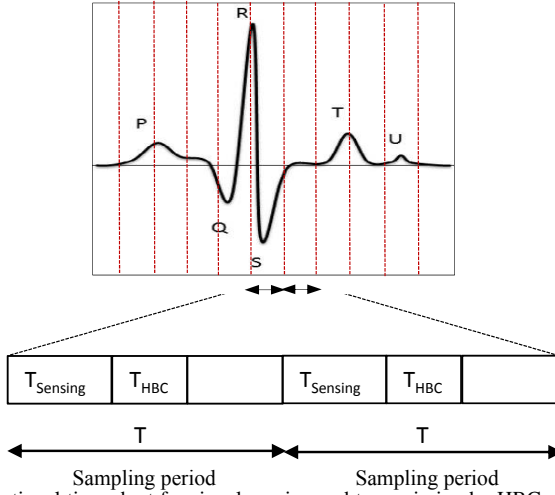


Fig. 7. Conceptual time chart for signal sensing and transmission by HBC-based ECG.

satisfy this path loss requirement in order to assure a reliable communication for vital signal transmission.

We then connected the transmitter and receiver with a programmable attenuator by coaxial cables to evaluate the bit error rate (BER) performance as a function of path loss. Fig. 8 shows the measured BER versus attenuation. As can be seen, when the AGC works well, the BER can be in the order of  $10^{-4}$  up to 82 dB attenuation. Even if the attenuation is increased to 85 dB, an BER of  $10^{-3}$  can still be achieved. Such an attenuation covers the path loss on the entire upper part of human body. For the transmission from feet to hand, the path loss may be estimated in the order of 80 dB from the simulated results in [16]. Since our transceiver can achieve a BER smaller than  $10^{-3}$  up to 85 dB attenuation, it should be still possible to receive the data by touching the hand on the receiver. Actually, in [12], an HBC communication from feet to the upper body has been demonstrated for an automated ticket gate.

As a realistic scenario of vital signal transmission, we further conducted a data transmission experiment through the human body for three subjects. As shown in Fig. 9, the transmitter was attached on the human chest. The digital data were transmitted from the transmitter on the chest to a fingertip. The fingertip touched the receiver which was connected to a PC via USB interface for recording the received data and counting the BER. The PC and receiver were battery-powered, and the system works continuously at least six hours. The measured BER performances were tabulated in Table II. It can be seen that the average BER is  $1.2 \times 10^{-3}$ . Such a BER level is acceptable in the physical layer design, because it can provide an error-free communication after employment of forward error correction. So the IR-type HBC transceiver exhibits a sufficient feasibility to realize the vital signal transmission at a data rate as high as 1.25 Mbps.

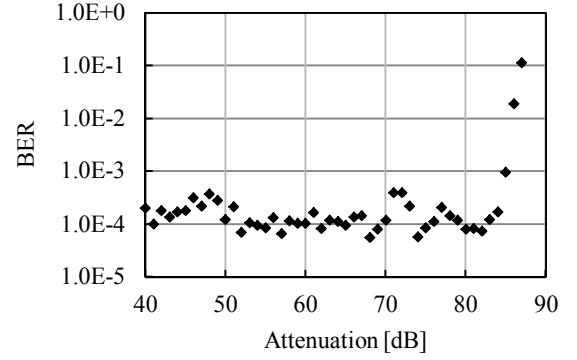


Fig. 8. Measured BER as a function of attenuation.

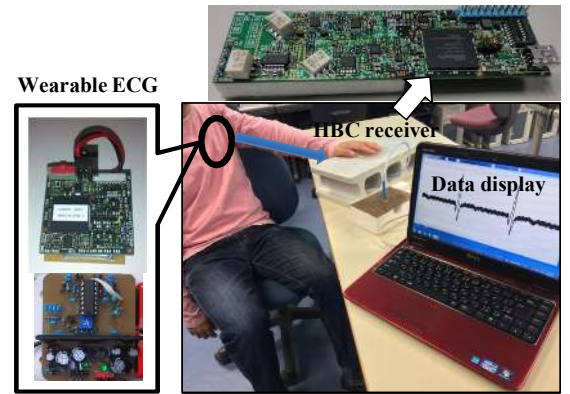


Fig. 9. View of measurement for vital data transmission from the chest to a fingertip.

#### IV. ECG PERFORMANCE EVALUATION

In order to verify the validity of the HBC-based wearable ECG, we compared its performance with both a commercially available radio-frequency (RF) ECG [8] and a wearable Holter ECG. ECG signals are usually used for heart rate variability (HRV) analysis. HRV is a physiological phenomenon of variation in the time interval between heartbeats. It is measured by the variation in the beat-to-beat interval. In the time domain, the representative parameters are RR interval (RRI), RR50 and the standard deviation of RRI (SDNN). RRI is the time between beats used to calculate heart rate. RR50 is the ratio of the number of adjacent intervals differing by over 50 ms in one-minute period. In the frequency domain, the representative parameters are low frequency heart rate fluctuation (LF), high frequency heart rate fluctuation (HF) and LF/HF ratio. The comparison results are shown as follows.

TABLE II  
MEASURED BER FROM THE CHEST TO A FINGERTIP

Subject 1	Subject 2	Subject 3	Average
$0.7 \times 10^{-3}$	$0.5 \times 10^{-3}$	$2.4 \times 10^{-3}$	$1.2 \times 10^{-3}$

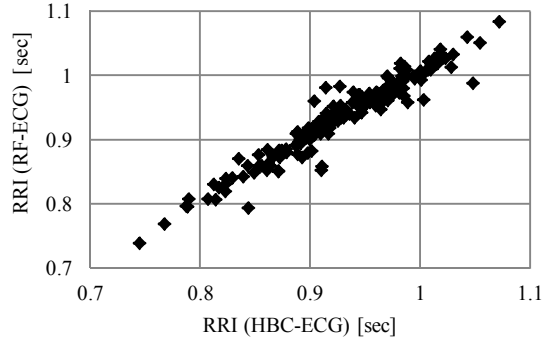


Fig. 10. HBC-ECG-acquired RRI versus RF-ECG-acquired RRI.

TABLE III  
COMPARISON OF RR50 [SAMPLE/MIN] BETWEEN HBC-ECG AND RF-ECG

	A	B	C	D	E	F
HBC-ECG	12	16	12	15	13	11
RF-ECG	15	13	14	14	14	11
Diff. (%)	20.0	23.1	14.3	7.1	7.1	0.0

#### A. Comparison with RF-ECG

The RF-ECG employs a narrow band modulation scheme at 2.4 GHz for transmitting ECG data to a PC. The ECG data are sampled with a sampling frequency of 204 Hz and transmitted at a data rate of 1 Mbps and an output power of 1 mW. The dimensions of the RF-ECG are  $40 \times 35 \times 7.2$  mm. We set both our HBC-based wearable ECG and the RF-ECG on the chest with an adequate spacing, and in both cases the receivers were connected to a PC via USB interface. In the HBC-based ECG case, the ECG data were transmitted to the PC when the left hand touched the receiving electrode in the receiver. While in the RF-ECG case, the ECG data were transmitted to the PC by 2.4 GHz wireless communication. The ECG measurement and transmission were conducted for six subjects, and each measurement lasted five minutes. Fig. 10 shows the HBC-ECG-acquired RRI versus RF-ECG-acquired RRI. They are in good agreement with an correlation coefficient larger than 0.93. Tables III and IV compare the derived RR50 and SDNN between the HBC-based ECG and RF-ECG for the six subjects. The relative differences are found ranging from 0% to 23.1% for RR50, and from 0% to 18.6% for SDNN, respectively. These results demonstrate that the HBC-based ECG provides almost equal performance as the commercially available RF-ECG in the time domain.

Moreover, we also obtained the power spectrum of RRI data with Fourier transform. Fig. 11 compares the results between HBC-based ECG and RF-ECG. The spectrum components

TABLE IV  
COMPARISON OF SDNN [MS] BETWEEN HBC-ECG AND RF-ECG

	A	B	C	D	E	F
HBC-ECG	69	51	69	53	66	41
RF-ECG	66	43	69	49	67	39
Difference (%)	4.5	18.6	0.0	8.2	1.5	4.9

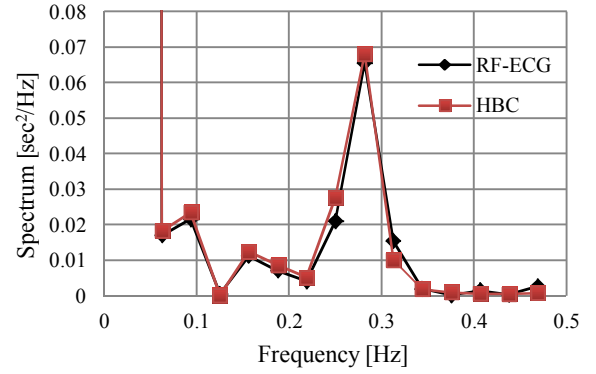


Fig. 11. Comparison of RRI power spectra between HBC-based ECG and RF-ECG.

TABLE V  
COMPARISON OF LF/HF BETWEEN HBC-ECG AND RF-ECG

	A	B	C	D	E	F
HBC-ECG	5.53	0.31	1.86	0.51	2.29	0.39
RF-ECG	5.42	0.31	1.47	0.42	2.14	0.46
Difference (%)	2.0	0.0	26.5	21.4	7.0	15.2

are found to mainly locate at LF range (from 0.05 to 0.15 Hz) and HF range (from 0.15 to 0.4 Hz) in both cases. Table V compares the ratio of the integration values of power spectra between LF range and HF range (LF/HF). The relative difference ranges from 0% to 26.5%, which confirms the validity of our HBC-ECG also in the frequency domain.

#### B. Comparison with Holder ECG

The validity of the HBC-based ECG was further verified by comparison with a Holter ECG (Fukuda Denshi) which continuously records the heart's rhythms as medical equipment. We set both the HBC-based ECG and Holter ECG on the chest, and measured the RRI, RR50, SDNN and LF/HF during five minutes for three subjects, respectively. The HBC-ECG-acquired data were sent to a PC in real time, and the Holter-ECG-acquired data were recorded by itself. Tables VI - IX compare the obtained results. As can be seen, the correlation coefficient between the HBC-based ECG and the Holter ECG is higher than 0.95, and the relative differences for RR50, SDNN and LF/HF are within 8.8%, 3.3% and 4.9%, respectively. These results strongly support that our HBC-based ECG has the almost same accuracy as the medical ECG equipment. They also show that the HBC-based ECG can provide more accurate ECG characteristics than the RF-ECG, because the relative differences from the Holter ECG are smaller. With respect to that the RF-ECG sends the data by 2.4 GHz wireless technology and the Holter ECG records the data in a recorder, the HBC-based ECG can send unconsciously the data to a PC or tablet by HBC technology in real time and high security.

#### C. In-Car Use of HBC-based ECG

As a scenario of possible applications, the feasibility of HBC-based wearable ECG was examined in a driving car. The

TABLE VI  
CORRELATION COEFFICIENT BETWEEN HBC-ECG AND HOLTER ECG

A	B	C
0.953	0.984	0.972

TABLE VII  
COMPARISON OF RR50 [SAMPLE/MIN] BETWEEN HBC-ECG AND HOLTER ECG

	A	B	C
HBC-ECG	18.8	12.3	7.8
Holter ECG	17.7	11.3	8.3
Difference (%)	6.2	8.8	6.0

subject wearing the HBC-based ECG sat in the front seat of the car. The HBC receiver was placed before the front glass and connected to a PC next to it by USB cable. While the subject was touching the receiver, the ECG data were continuously sent to the PC, in which we incorporated a program to extract the received ECG waveform with a moving average filter and simple error correction technology, and display it in real time. Fig. 12(a) and (b) show the ECG transmission in a driving car and the received ECG time waveform in the PC, respectively. Not only the QRS-wave but also the P-wave and T-wave can be clearly observed in the received ECG waveform. This result sufficiently shows the feasibility of the HBC-based ECG in actual applications.

## V. CONCLUSIONS

HBC has attracted much attention in wireless BANs for healthcare, medical and entertainment applications because of its low path loss and high security characteristics. In this study, we have developed a wearable ECG based on wide band IR-type HBC technology for transmitting vital sign signals in real time. The wide band feature of the IR-type HBC transceiver has contributed to make it satisfy the extremely weak radio laws without license requirement, and the BER smaller than  $10^{-3}$  has shown a sufficiently good physical layer performance for on-body transmission at a data rate as high as 1.25 Mbps. Moreover, the common use of sensing and transmitting electrodes has largely simplified the structure of the wearable ECG. For verifying the validity of the HBC-based wearable ECG, we have compared it with both a commercially available RF-ECG and a wearable Holter ECG. The comparison results

TABLE VIII  
COMPARISON OF SDNN [MS] BETWEEN HBC-ECG AND HOLTER ECG

	A	B	C
HBC-ECG	63	70	60
Holter ECG	61	69	60
Difference (%)	3.3	1.4	0.0

TABLE IX  
COMPARISON OF LF/HF BETWEEN HBC-ECG AND HOLTER ECG

	A	B	C
HBC-ECG	0.76	1.86	1.51
Holter ECG	0.73	1.78	1.44
Difference (%)	4.1	4.5	4.9

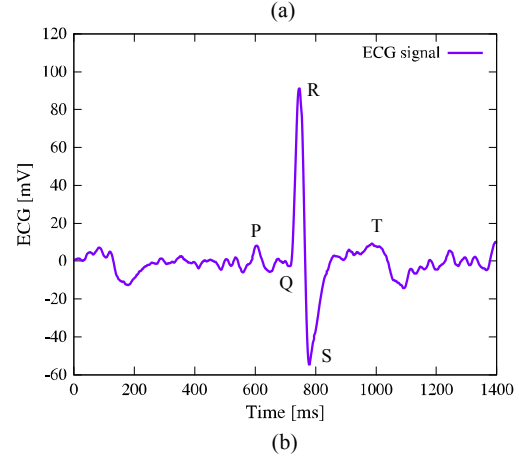


Fig. 12. (a) ECG signal transmission by HBC-based wearable ECG in driving car, (b) received ECG waveform in PC.

for various ECG parameters in time domain and frequency domain have shown good agreement with both the RF-ECG and Holter ECG. The correlation coefficients for RRI have been found as high as 0.93 for RF-ECG and 0.95 for Holter ECG. The good agreement especially with the Holter ECG strongly support the validity of the developed HBC-based ECG. The successful use of the HBC-based ECG in a driving car has also demonstrated its feasibility in actual scenarios. This should be the first time to have successfully applied the HBC technology in real time ECG monitoring.

A future subject is to integrate various vital sign sensors in the HBC transceiver for various multiple sensor scenarios.

## ACKNOWLEDGMENT

This study was supported in part by JSPS Grants-in-Aid for Scientific Research Grant Number 15H04006.

## REFERENCES

- [1] IEEE Std 802.15.6-2012: IEEE Standard for local and metropolitan area networks – Part 15.6: Wireless Body Area Networks, Feb. 2012.
- [2] J. Wang and Q. Wang, Body Area Communications, Wiley-IEEE, 2013.
- [3] P. Bonato, "Wearable sensors and systems - From enabling technology to clinical applications", IEEE Eng. Med. Biol. Mag., vol.29, no.3, pp.25-36, May/June 2010.
- [4] E. Nemati, et al., "A wireless wearable ECG sensor for long-term applications", IEEE Commun. Mag., pp. 36-43, Jan. 2012.
- [5] N. Guler and U. Fidan, "Wireless transmission of ECG signal," J. Med. Syst., vol. 30, pp. 231-236, 2006.
- [6] C. Lin, et al, "An intelligent telecardiology system using a wearable and wireless ECG to detect atrial fibrillation", IEEE Trans. Inf. Technol. in Biomedicine, vol. 14, no. 3, pp. 726-733, May 2010.

- [7] J. Gomez-Clapers and R. Casanella, "A fast and easy-to-use ECG acquisition and heart rate monitoring system using a wireless steering wheel", *IEEE Sensors Journal*, vol.12, no.3, pp. 610-616, March 2012.
- [8] Online Available: [http://www.mmdevice.co.jp/english/goods\\_01.html](http://www.mmdevice.co.jp/english/goods_01.html)
- [9] T. G. Zimmerman, "Personal area networks: Near-field intrabody communications", *IBM Syst. J.*, vol. 35, no. 3 & 4, pp. 609-617, 1996.
- [10] M. Shinagawa, et al., "A near-field-sensing transceiver for intrabody communication based on the electro-optic effect," *IEEE Trans. Instrum. Meas.*, vol. 53, no. 12, pp. 1533-1538, Dec. 2004.
- [11] H. Baldus, et al., "Human-centric connectivity enabled by body-coupled communications", *IEEE Commun. Mag.*, pp. 172-178, June 2009.
- [12] Y. Kado and M. Shinagawa, "AC electric field communication for human-area networking", *IEICE Trans. Electron.*, vol. E93-C, no. 3, pp. 234-243, March 2011.
- [13] K. Shikada and J. Wang, "Development of human body communication transceiver based on impulse radio scheme", *Proc. IEEE CPMT Symp.*, Kyoto, Japan, Dec. 2012, pp.283-286.
- [14] M. Seyedi, et al., "An energy-efficient pulse position modulation transmitter for galvanic intrabody communications", *Proc. 4th Int. Conf. on Wireless Mobile Commun. & Healthcare*, Athens, Greece, Nov. 3-5, 2014, pp. 192-195.
- [15] Online Available: <http://www.tele.soumu.go.jp/j/ref/material/rule/> (in Japanese).
- [16] J. Wang, Y. Nishikawa and T. Shibata, "Analysis of on-body transmission mechanism and characteristic based on an electromagnetic field approach", *IEEE Trans. Microwave Theory Tech.*, vol. 57, no. 10, pp. 2464-2470, Oct. 2009.